COPERNICUS 940820 - TECHNICAL REPORT

Mathematical Modelling of the Effects of Mining at the Deposit Dolní Rožínka.

Software testing and computational results.

R. Blaheta, O. Jakl, R. Kohut, A. Kolcun, J. Malík, Z. Rakowski[1]
and A. Hájek [2]

Abstract: The paper describes mathematical modelling of the geomechanical effects of mining at the uranium deposit Dolní Rožínka. The modelling addresses many interesting topics as for example: modelling of complex process of mining with caving, modelling of complex pre-mining stress state, large scale 3D modelling, solution of pure Neumann problems of elasticity, iterative solution of large singular positive semidefinite systems, parallel computations. The paper includes directions for a further research.

[1]Institute of Geonics AS CR, Studentská 1768, 708 00 Ostrava–Poruba, Czech Republic
Supported by Grant COPERNICUS 940820 of the European Commission and Grant GA ČR 105/95/1273 of the Grant agency of the Czech Republic.
[2]GEAM, 592 61 Dolní Rožínka, Czech Republic. Supported by Grant COPERNICUS 940820 of the European Commision.

Contents

1 Introduction

This report describes mathematical modelling of the geomechanical effects of the uranium ore mining at the deposit D. Rožínka, see [11] for further details. This modelling has three main goals:

- to model influence of the mining process (overhand stoping with caving) on the rock mass which is important for the operation, safety and economy of the mine,
- to show requirements for extremely large 3D mathematical modelling for solving the stability and safety problems in mining industry,
- to test efficiency of the exploited software including the high performance solvers developed under the grants COPERNICUS 94 0820 and GAČR 105/95/1273.

The mathematical modelling of the mining effects at the deposit D. Rožínka was accompanied by in situ measurements of the pre-mining stress field carried out by the Department of Geomechanics of the Institute of Geonics, Ostrava, see [15].

2 Modelling of the mining process

In this Section, we describe main features of the modelled situation and the mining process of ore extraction with caving. We also outline the methodological approach which will be used for the mathematical modelling. Finally, we shall formulate the main aims of the modelling.

Basic situation

Roughly speaking, we are interested in the effects caused by mining in a part of the uranium ore deposit at Dolní Rožínka. The domain of direct interest has the dimensions 630x335x330 metres, is located in the depth of 900 metres under the surface and contains a 145 metres wide zone with three uranium ore veins. This domain with the adopted coordinate system and its orientation can be seen from Figure 2.1.

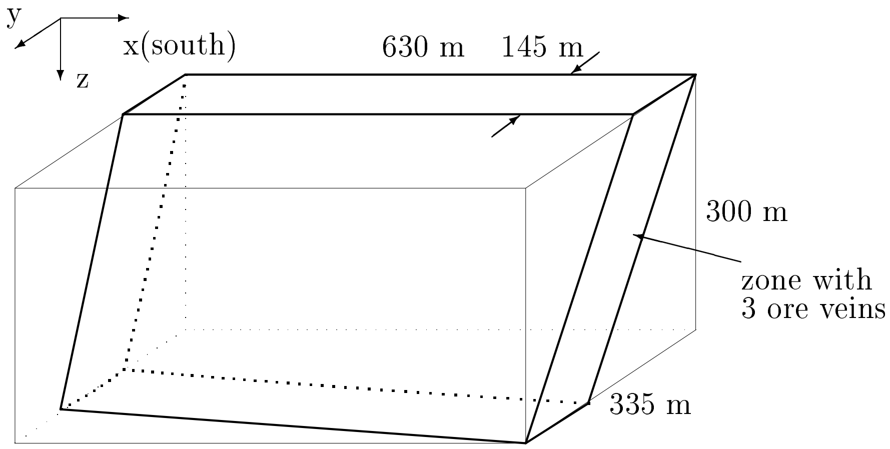

Figure 2.1: Domain of interest and the coordinate system.

Pre-mining state of stress

According to the performed in situ measurements [15], the pre-mining stress shows a substantial anisotropy in the horizontal planes and the values which substantially differ from the frequently used values which correspond to the stress state induced only by weight in an elastic rock mass.

As a first choice, we shall consider the horizontal stresses according to Figure 2.2. This means that in the horizontal plane we have two principal stresses

$$\sigma_1 = 2 s_{zz}\,, \quad \sigma_2 = 0.5\, s_{zz}$$

where s_{zz} is the vertical stress computed according to the formula

$$s_{zz} = -\gamma\, h$$

where γ is the (averaged) unit weight of rock and h is the depth under surface. The principal stresses can be related to the stress components w.r.t. the adopted coordinate system by the relations

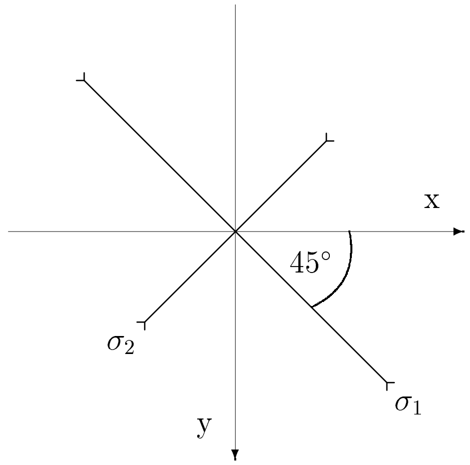

Figure 2.2: Pre-mining stress field. Orientation of the principal stresses σ_1, σ_2 in the horizontal plane.

$$S_H\, d_i \;=\; \sigma_i\, d_i \quad i \;=\; 1, 2$$

where

$$S_H \;=\; \begin{bmatrix} s_{xx} & s_{xy} \\ s_{xy} & s_{yy} \end{bmatrix}, \quad d_i \;=\; \begin{bmatrix} \cos\alpha_i \\ \sin\alpha_i \end{bmatrix},$$

$\alpha_1 \;=\; 45^\circ\,, \qquad \alpha_2 \;=\; -45^\circ\,.$

The above relations enable us to compute the stress components with respect to the adopted coordinate system. In this way, we obtain

$$s_{xx} \;=\; k_{xx}\, s_{zz}, \quad s_{xy} \;=\; k_{xy}\, s_{zz}, \quad s_{yy} \;=\; k_{yy}\, s_{zz} \tag{1}$$

where

$$k_{xx} \;=\; k_{yy} \;=\; 1.25 \quad \text{and} \quad k_{xy} \;=\; 0.75. \tag{2}$$

Note that the above choice of the pre-mining stress corresponds to the most extreme measured values. In a further plan, we will test the sensitivity of the results to the pre-mining stress values.

Modelling of the mining process

The uranium ore is mined out by the method of underhand stoping with caving, see [11]. This means that we should simulate relatively complex process of stage by stage extracting of the ore accompanied by damaging the rock in a zone adjacent to the openings. The excavation and the adjacent volume of fractured rocks are caved by the caving waste material.

In the case of mining without caving and without any filling of the extracted volumes in an elastic rock mass, the stress in the vicinity of the mine openings can be computed by the *incremental change modelling method.* It starts from the given pre-mining stress, compute sequentially loading on the surface of new openings induced by the initial stress and compute the stress increments and new stress state. If the pre-mining stress results as the solution of the boundary value problem in the considered domain then we can superpose this boundary value problem with the boundary value problem for computation of the stress increment. This gives the *global change modelling method* which computes the total stress for a given stage of mining by applying the forces, which would cause the pre-mining stress in the problem domain unaffected by mining, to the domain affected by the mining process.

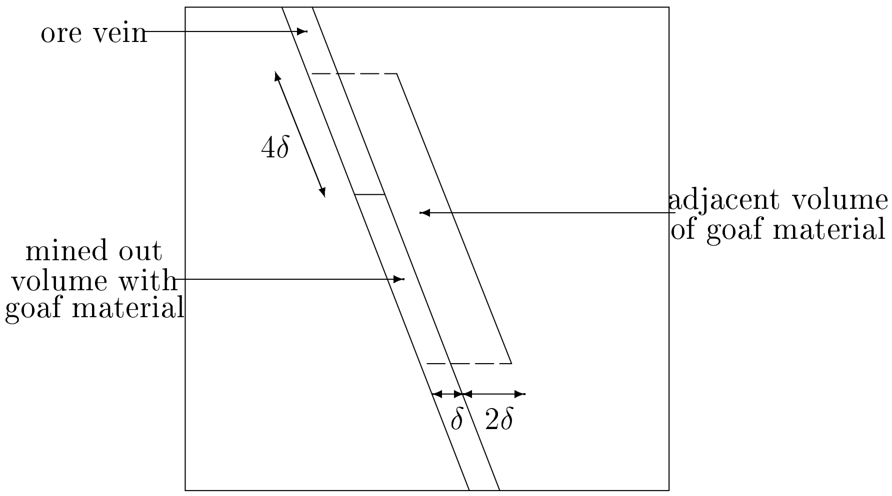

Figure 2.3: Dimensioning of the caved volume.

For the modelling of the mining technology with caving, we can adapt the global change modelling method. For a given stage of mining, we apply the forces to the domain containing volumes filled by the goaf material. These volumes consist of the really mined out parts and the adjacent zones of the fractured material; the mutual proportions of these parts can be seen from Figure 2.3.

With respect to the aims of the modelling, we shall consider four different stages of mining in the considered domain. An illustration of these stages can be seen from Figure 2.4.

Note that some attempt to use the incremental change modelling method for the case of mining with caving can be found in [10]. Due to methodological difficulties and unsatisfactory results, we have abandoned this approach for present, i.e. we shall use the global change modelling method throughout this paper.

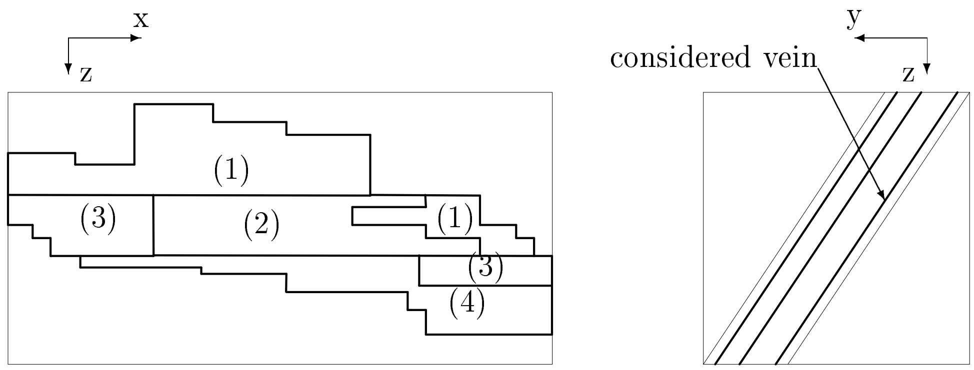

Fig. 2.4: Four stages of the mining process in one of three ore veins. (1) - the oldest mining stage, ..., (4) - the newest mining stage.

Aims of the modelling

In this paper, we shall concentrate on the following topics:

- zones of influence of the mining and mutual influence of mining in adjacent ore veins,
- stability of the mine openings,

- inclination to rock bursts.

The assessment of the above topics will be based on computation of the stress and strain fields in the vicinity of the mine openings. For the investigation of stability, we shall compare the near field stresses in various stages of mining. For the assessment of possibility of rock bursts, we shall watch the concentrations of the stresses and the strain energy in the hard rocks.

3 Mathematical formulation

To compute the stress field in the considered domain, we have to formulate a boundary value problem. To this end, we have to specify the problem domain, the boundary conditions, the volume load and the material behaviour. This specification will follow the considerations done in the previous Section.

Problem domain

We will formulate the boundary value problem in the domain Ω, which will be a sufficiently large parallelepiped containing the whole considered part of the deposit. Moreover, the problem domain must be sufficiently large to guarantee that the stress field is not influenced by the mining activities on the domain boundary, see further subsection devoted to the boundary conditions. In our case, the size of the problem domain will be 1430x550x600 metres with the top side situated horizontally in the depth of 800 metres under surface. This domain arises by enlarging the domain of interest, see Fig 2.1, by the following way:

$$\begin{aligned} 1\,430\ \mathrm{m} &= 200 + 630 + 600\ \mathrm{m} \\ 550\ \mathrm{m} &= 100 + 335 + 115\ \mathrm{m} \\ 600\ \mathrm{m} &= 100 + 300 + 200\ \mathrm{m}. \end{aligned}$$

This shows that the enlarging is not uniform and symmetric, but corresponding to the characteristics of the solved problem.

Sufficiency of the enlarging of the domain of interest can be seen from the behaviour of the computed stresses or from comparison with the solution from even larger computational domain.

Boundary conditions and volume loading

Boundary conditions on the (outer) boundary of the problem domain will be specified to simulate the actions of the surrounding rock mass, existing in the pre-mining stress state, to the problem domain. Note that the problem domain is assumed to be sufficiently large to guarantee that the surrounding rocks are in the pre-mining stress state.

The specified boundary conditions represent surface forces depending on the pre-mining stress state, i.e. on the depth h under the surface. The values of the boundary conditions are given in Table 3.1 where γ is the (averaged) unit weight of the material, k_{xx}, k_{yy} and k_{xy} are the coefficients from (2).

side		outer normal	depth h	surface force
top	z = 0	(0,0,-1)	$h =$ 800	$(0, 0, 1)\,\gamma h_0$
bottom	z = 600	(0,0,1)	$h =$ 1400	$(0, 0, -1)\,\gamma h$
east	y = 0	(0,-1,0)	$h = h_0 + z$	$(k_{xy}, k_{yy}, 0)\,\gamma h$
west	y = 600	(0,1,0)	$h = h_0 + z$	$-(k_{xy}, k_{yy}, 0)\,\gamma h$
north	x = 0	(-1,0,0)	$h = h_0 + z$	$(k_{xx}, k_{xy}, 0)\,\gamma h$
south	x = 1430	(1,0,0)	$h = h_0 + z$	$-(k_{xx}, k_{xy}, 0)\,\gamma h$

Table 3.1: Boundary conditions.

Note that the adopted, the pure force (Neumann - type) boundary conditions, are not standard for the FE analysis based on the displacement formulation. Usually the forces on some side of the problem domain are replaced by reactions of a rigid support arising from fixing the normal component of displacement. Due to more complicated character of the pre-mining stress field, any such fixing causes relatively large disturbations of the stress field and therefore, we finally adopt the pure Neumann - type boundary conditions.

The volume loading is given by the weight of the materials, see Table 3.2.

Note that by considering two different unit weights for the rock and the goaf, we obtain a slight violation of consistency in the formulated boundary value problem. By consistency, we mean here that the resultants of all external load forces as well as all moments vanish. This may be overcome by using the same unit weight for goaf and rocks or by finding (only) generalized solution of the problem. The later approach will be used in the reported modelling.

Material behaviour

The problem domain not influenced by the mining activities consists of two basic materials: the uranium ore and the surrounding rock which have the same mechanical behaviour, see Table 3.2.

	Elasticity modulus [MPa]	Poisson ratio	Unit mass $[g/cm^3]$
rock massif	20 000	0.25	2.7
uranium ore	20 000	0.25	2.7
goaf	2 500	0.4	2.0

Table 3.2: Material parameters.

According to the adopted global change modelling procedure, we must describe also the behaviour of the caved waste (goaf) material. Here, we can consider a nonlinear behaviour with the material parameters depending on the deformation or density, see [17]. Because have had no experimental data for the description of nonlinear behaviour of the goaf, we assume again linear behaviour of this material, see Table 3.2. Note that a positive experience with this simplification was gained during the 2D modelling, cf. [16].

The goaf material is assumed in regions which consist of the excavated volumes and their neighbourhoods, see Figure 2.3.

Pure Neumann BVP of elasticity

The adopted method of the modelling of effect of the mining process leads to formulation of a boundary value problem (BVP) of elasticity with pure Neumann-type boundary conditions. This BVP can be written in the form

$$\sum_{i=1}^{3} \frac{\partial \sigma_{ij}}{\partial x_j} + f_i^v = 0 \qquad \text{in} \quad \Omega, \tag{3}$$

$$\sigma_{ij} = \sum_{k,l=1}^{3} c_{ijkl}\, \varepsilon_{kl} \qquad \text{in} \quad \Omega, \tag{4}$$

$$\varepsilon = \varepsilon(u) = (\varepsilon_{ij}) \qquad \text{in} \quad \Omega, \tag{5}$$

$$\varepsilon_{ij} = \frac{1}{2}\left(\frac{\partial u_i}{\partial x_j} + \frac{\partial u_j}{\partial x_i}\right) \qquad \text{in} \quad \Omega \tag{6}$$

$$\sum_{i=1}^{3} \sigma_{ij} n_j = f_i^s \qquad \text{on} \quad \partial\Omega \tag{7}$$

Above, $u : \Omega \to R^3$ denotes the displacement, $\sigma = (\sigma_{ij})$ denotes the stress tensor, $\varepsilon = (\varepsilon_{ij})$ denotes the small strain tensor, $n = (n_1, n_2, n_3)$ is the unit outer normal to Ω, $\partial\Omega$ denotes the boundary of Ω. The constants c_{ijkl} are the material characteristics. For isotropic materials, the constants c_{ijkl} can be expressed in terms of the elasticity modulus and the Poisson ratio. The functions f_i^v and f_i^s describe densities of the volume (weight) and surface forces, respectively. For all details, see [19].

We use the formulation in displacement although we are interested here only in stresses. In this respect, the important feature of the pure Neumann BVP is that the displacement is not determined uniquely. More precisely, the displacement is determined up to a rigid-body displacement (translation or rotation). These rigid-body displacements form a space V_0 with a basis given by the functions

$$w_1(x) = \begin{pmatrix} 1 \\ 0 \\ 0 \end{pmatrix}, \; w_2(x) = \begin{pmatrix} 0 \\ 1 \\ 0 \end{pmatrix}, \; w_3(x) = \begin{pmatrix} 0 \\ 0 \\ 1 \end{pmatrix}, \tag{8}$$

$$w_4(x) = \begin{pmatrix} 0 \\ -x_3 \\ x_2 \end{pmatrix}, \; w_5(x) = \begin{pmatrix} -x_3 \\ 0 \\ x_1 \end{pmatrix}, \; w_6(x) = \begin{pmatrix} -x_2 \\ x_1 \\ 0 \end{pmatrix}. \tag{9}$$

Because the rigid body displacement give zero strains and stress, the stress will be determined uniquely.

The solution of the pure Neumann BVP of elasticity exists only if the resultants of all forces and moments vanish, i.e. if

$$\int_\Omega f_i^v \, dx + \int_{\partial\Omega} f_i^s \, ds = 0, \qquad i = 1, 2, 3$$

$$\int_{\Omega} x \otimes f_i^v \, dx + \int_{\partial\Omega} x \otimes f_i^s \, ds \, = \, 0 \, , \qquad i = 1, 2, 3$$

where $\otimes$ is the vector product in R^3. The above conditions which are called conditions of consistency, can be interpreted also as orthogonality, see again [19] and the discussion in the next Section.

The conditions of consistency, may be violated if we consider different unit weights of rock and goaf material without reflecting it in the specified boundary conditions. In such case, we can find the generalized solution, i.e. the solution of the problem with a modified loading. We shall discuss the details in the contents of the finite element method in the next Section.

Stress characteristics

For the assessment of the effects of mining we shall use components of the stress tensor

$$\sigma \, = \, \begin{bmatrix} s_{xx} & s_{xy} & s_{xz} \\ s_{xy} & s_{yy} & s_{yz} \\ s_{xz} & s_{yz} & s_{zz} \end{bmatrix} .$$

and the following derived quantities.

The *mean stress* s_m ,

$$s_m \, = \, \frac{1}{3} \left(s_{xx} + s_{yy} + s_{zz} \right) \, ,$$

the *shear stress intensity* s_i ,

$$s_i \, = \, \Big[\frac{(s_{xx} - s_{yy})^2}{6} + \frac{(s_{yy} - s_{zz})^2}{6} + \frac{(s_{xx} - s_{zz})^2}{6} + s_{xy}^2 + s_{yz}^2 + s_{zx}^2 \Big]^{1/2} \, ,$$

and the *tensile stress indicator* t_i,

$$t_i \, = \, \{ \delta_1 \, \geq \, 0 \text{ .OR. } \delta_2 \, \leq \, 0 \text{ .OR. } \delta_3 \, \geq \, 0 \} \, \in \, \{\text{TRUE}, \text{FALSE}\}$$

where δ_1, δ_2 and δ_3 are principal subdeterminants (minors) of σ. Here t_i is a logical value computed on the basis of Sylvestr's criterion indicating the state of negative semidefiniteness of σ which corresponds to state without tensile stress. More precise analysis can be done on the basis of principal stresses.

The zones of stress and strain energy concentration can be evaluated by means of the strain energy density E,

$$E = \sigma^T \varepsilon = \varepsilon^T D \varepsilon = \sigma^T D^{-1} \sigma^T$$

where σ, ε are vectors of stress or strain tensor components and D is the Hooke's matrix given by the relation (4). Note that $\sqrt{E}$ gives also a norm of the strains or the stresses.

4 Numerical solution

Finite element analysis

For the finite element (FE) analysis, we shall use the linear tetrahedral finite elements. The problem domain is firstly decomposed into hexahedral (not necessary rectangular) bricks which are further decomposed, each brick into six tetrahedra.

For testing proposes, we have prepared a FE grid of 28 x 35 x 32 nodes (small Rožínka model).

For the modelling, we have used finer FE grid of 124 x 137 x 76 nodes which is relatively fine in the area of interest. Here we can find the smallest bricks of 8 x 1 x 5 metres.

In the area outside the domain of interest the grid is gradually coarsened. The coarsening is not very high to avoid the appearance of elements with very high aspect ratio.

For the future, we plan to use composite grid formulation which enables

- efficient coarsening of the grid outside the domain of interest,
- efficient modelling of details.

Grid generation

The division of the computational domain into hexahedral bricks is defined by a deformation of uniform rectangular grid. Firstly, some "index" planes are deformed by using three tools: prescribing position of some nodes; interpolation

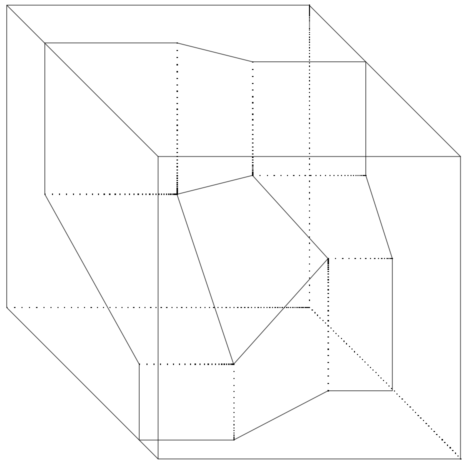

Figure 4.1: Deformation of an "index" plane.

within the index rectangle; projections to the boundary. These tools can be seen from Figures 4.1 and 4.2. Secondly, other "index" planes are embedded among the previously defined ones and nodes on these planes are computed by interpolation.

Deformation of an index plane and a surface view on the coarser 28x35x32 node computational grid for the small Rožínka model can be seen from Figures 4.2 and 4.3. The view on the finer 124 x 137 x 76 node grid is very similar, but due to the density this grid it can not be shown in a similar small format.

Iterative solution of the FE systems

The finite element analysis of pure Neumann BVP of elasticity leads to the linear system

$$Au = b\,, \quad u, b \in R^n \tag{10}$$

where A is a *singular*, positive semidefinite, symmetric $n \times n$ matrix.

The question, which arises due to singularity of the matrix A, is whether the system (10) can be solved by the existing solvers [5], [7] based on the preconditioned conjugate gradient method with preconditioning given by the displacement decomposition - incomplete factorization technique, see [4]. This question will be discussed in this Subsection.

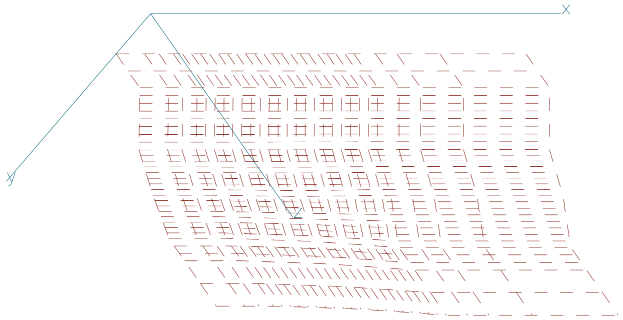

Figure 4.2: Deformation of an "index" plane for the small Rožínka model.

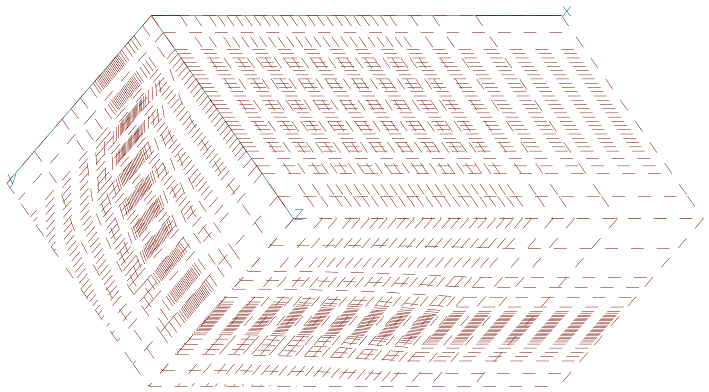

Figure 4.3: FE grid for the small Rožínka model.

Consistency

Due to symmetry of A, the space R^n can be decomposed as

$$R^n = R(A) \oplus N(A)\,,$$

where $R(A)$ is the range and $N(A)$ is the null space of the matrix A.

We say that the right hand side b of (10) is *consistent* if $b \in R(A)$. For the consistent rhs b, there exists a solution of (1) which is not unique.

For a general rhs b, the rhs can be decomposed into consistent and inconsistent parts, $b = \bar{b} + \tilde{b}$, $\bar{b} \in R(A)$, $\tilde{b} \in N(A)$. Any solution of $Au = \bar{b}$ is then called the *generalized solution* of (10).

Convergence of the CG method

The conjugate gradient (CG) method can be applied also to the solution of the singular systems. We can distinguish three cases, cf. [1], [2].

- b is consistent and the initial guess $u_0 \in R(A)$. In this case all vectors generated by the CG algorithm remains in R(A) and the CG algorithm is equivalent to the CG algorithm for the system with operator $\bar{A}$ which is the restriction of A to $R(A)$. The convergence of the CG method is given by the spectrum $\sigma(\bar{A}) = \sigma(A) \setminus \{0\}$.

- b is consistent, $u_0 = \bar{u}_0 + \tilde{u}_0$, $\bar{u}_0 \in R(A), \tilde{u} \in N(A)$. The CG method now gives iterations $u_i = \tilde{u}_0 + \bar{u}_i$, where $\bar{u}_i$ are the iterations which would be obtained when we started the CG algorithm with the initial guess $\bar{u}_0$.

- b is *inconsistent*. In this case the CG method may not converge, see [1].

Preconditioning

We shall consider the preconditioner of the form

$$C = (X + L)X^{-1}(X + L)^T \tag{11}$$

where L is the strictly lower triangular part of the matrix $\tilde{A}$ which is the separate displacement component part of A, see [4] and [5]. Here, X is a diagonal matrix determined by requirement of equal rowsums,

$$\mathrm{rowsum}\,(C) = \mathrm{rowsum}\,(\tilde{A} + \tilde{D}) \tag{12}$$

where $\tilde{D} > 0$ is a suitable diagonal perturbation of $\tilde{A}$, see again [4].

The matrix $\tilde{A}$ has zero rowsums because the rigid–body translations belongs to $N(\tilde{A})$. The lower triangular part of $\tilde{A}$ is not positive, $L \leq 0$, under the conditions which depend on the material characteristics and the shape of finite elements. In case of $L \leq 0$, we can prove that there is a positive $X > 0$ satisfying (12), see [4], Theorem 2.1.

Hence, the displacement decomposition – incomplete factorization technique can give a *regular preconditioner* C to A also in the case of the singular system (10). The preconditioned CG method can be viewed as the CG method applied to the transformed system

$$C^{-1/2}AC^{-1/2}\hat{u} = C^{-1/2}b \tag{13}$$

which is again singular. The transformed system is consistent if $b \in R(A)$.

More about the incomplete factorization preconditioners for singular positive semidefinite systems can be found in [18], [2].

Solution of slightly inconsistent systems

By slightly inconsistent systems, we shall understand the case when the right hand side b has nonzero but small inconsistent part,i.e.

$$b = \bar{b} + \tilde{b},\ \bar{b} \in R(A),\ \tilde{b} \in N(A),\ \tilde{b} \neq 0,\ \| \tilde{b} \| << \| b \| \ .$$

In this case we can use the following procedures.

- We can apply the preconditioned CG method directly to the slightly inconsistent system (10). We suppose that the CG process will be convergent in the initial phase and will be able to produce iteration u_i with a sufficiently small residual,

  $$\| Au_i - b \| < \varepsilon \ .$$

  Such iteration gives also an approximation to a generalized solution of (10) because, due to orthogonality of $R(A)$ and $N(A)$,

  $$\| Au_i - \bar{b} \|^2 \leq \| Au_i - \bar{b} \|^2 + \| \tilde{b} \|^2 = \| Au_i - b \|^2 \ . \tag{14}$$

- Second procedure consists in a modification of the right hand side by subtraction of the inconsistent part. To this end, we exploit the knowledge of the null space $N(A)$ which is created by the FE (grid) functions corresponding to the rigid–body displacements described in (8), (9).

For the systems arising from the modelling described in previous sections, the inconsistentness measured by the ratio $\| \tilde{b} \| \ / \ \| b \|$ was of order 10^{-5}. This enables to apply the preconditioned CG method directly (first procedure) for obtaining the solution within the accuracy $\varepsilon = 10^{-3}$ which was sufficient for our purposes. For obtaining more accurate solution of the linear systems, it was necessary to use the second procedure. Nevertheless, due to finite arithmetics, we were able to improve the consistency only to a limited value. For the small Rožínka model, we were able to compute the approximate solution only up to the accuracy $\varepsilon = 10^{-5}$.

5 Exploited software and computers

Programs

All computations were performed by using the following programs developed at the Department of Applied Mathematics of the Institute of Geonics:

TGRID-2 – preprocessor for regular not necessarily uniform or rectangular grids. The preprocessor creates files with information about nodes, elements, materials, boundary conditions. For a detailed description, see [14].

FEMSYS – system of codes for generation of the stiffness matrices for linear tetrahedral FE and assembling the global stiffness matrix and the global load vector, see [6], [13].

PCG-1 – linear system solver based on the conjugate gradient method with preconditioning by the displacement decomposition - incomplete factorization technique, see [5] and [4].

PCG-P – parallel version of the above solver for three processor computer systems, see [7].

STRESS – computation of stresses and strains, averaging of stress in hexahedral bricks.

GEMQ – interactive alphanumeric outputs, graphics outputs, query language, postprocessing.

Computers

The computations reported in this paper were performed on two computer systems: IBM RS/6000 model 3CT computer installed at the Institute of Geonics and IBM SP - 2 multiprocessor system installed at the VŠB - Technical

University of Ostrava. Both computers are based on the same microprocessor architecture which enables easy transfer of binary compatible codes. The computing power of IBM RS/6000 3CT computer is approximately equal to the power of each of the nodes of the IBM SP-2 system. The parameters of the computers can be seen from Table 5.1. Note that the parallel codes use the PVM (Parallel Virtual Machine) message passing environment and the HPS (High Performance Switch) interconnection network on the SP-2 system.

Specifications	*IBM RS/6000 3CT*	*IBM SP-2*
# processors	1	8
Processor type	POWER2/66.7 MHz	POWER2/66.7 MHz
System memory [MB]	128	128 (5x), 256 (3x)
Linpack DP [MFLOPS]	133	133
Disk storage [GB]	6.5	9
Interconnection network		High Perf. Switch
Latency (IP) [μs]		270
Bandwidth (IP) [MByte/s]		12
Operating system	AIX 3.2.5	AIX 4.1.3

Table 5.1: Parameters of the computers.

6 Characteristics of the computations

System memory requirements

The parameters of the solved FE problems with the finer 124 x 137 x 76 node grid are the following

	# nodes	= 1 291 088
NEQ =	# equations	= 3 873 264
NEL =	# elements	= 7 527 600

Disk memory requirements

Totally 1.735 GB.
The biggest demands come from the storage of the following files:

FEL (information about elements, size NEL * 76):	572 MB
FKBC (stiffness matrix, size NEQ * 168):	664 MB
FSTSV (stress and components, NEL * 48):	362 MB

Storage requirements for vectors like displacements, forces etc. are equal to 15.5 MB per 1 vector.

System memory requirements

FEMSYS (part of the stiffness matrix + 3 vectors + rest)	: $\sim$ 55 MB
PCG–1 (5 vectors + rest)	: $\sim$ 77.5 MB
STRESS (1 vector + rest)	: $\sim$ 15.5 MB

Computer time requirements

The elapsed computer time requirements can be seen from Table 6.1. The times reported for the PCG–P parallel solver concerns the computations on 3 processor nodes of the IBM SP–2 system, the other times were obtained on IBM RS/6000 3CT. As expected, the crucial times were consumed by the solvers.

	STAGE 1	STAGE 2	STAGE 3	STAGE 4
TGRID–2	00:10:39	00:04:14	00:04:20	00:04:11
FEMSYS	00:30:11	00:32:03	00:34:04	00:29:28
PCG–1	25:54:27	05:39:31	04:28:03	09:14:14
PCG–P	11:55:10	02:42:29	02:35:44	04:46:16
STRESS	00:09:25	00:09:35	00:09:30	00:09:28

Table 6.1: Computer (wall-clock) times.

The reported times correspond to the solution of linear systems with the accuracy given by the condition

$$\frac{l_2 - \text{norm of the residual}}{l_2 - \text{norm of the rhs}} < 10^{-3} .$$

Substantial amount of the computer work is saved in the modelling stages 2, 3 and 4 by taking the solution from the previous stage as an initial guess.

Note that both PCG–1 and PCG–P solvers use the same iterative technique which needs the following numbers of iterations (in four modelling stages):

$$172 + 36 + 28 + 60 = 296 \text{ iterations.}$$

The full convergence history can be found in Appendix 1.

An interesting feature can be also seen from the comparison of the times for the PCG-1 solver which were obtained when we solved the small Rožínka model and the large one (the computations were performed on IBM RS/6000 3CT).

- increase of the number of unknowns: $\sim$ 41 times,
- increase of the number of iterations: $\sim$ 2 times,
- increase of the computer time per 1 iteration: $\sim$ 256 times.

Theoretically, the computer time per 1 iteration depends linearly on the number of unknowns. This comparison shows that the operating system can optimize the computations including the input/output operations when the problem is not too large and motivates again the interest in problem decompositions and parallel computing.

7 Concluding remarks and directions for further research

This paper describes the development of a mathematical model for the assessment of effects of mining at D. Rožná deposit, the methods used for the numerical solution and characteristics of the performed computations. The engineering evaluation of the obtained results will be discussed in the next report concerning the role of large scale mathematical modelling in the development of new mining technologies.

Main conclusion from the presented results is that the development of high performance solvers together with the use of contemporary fast and parallel computer systems make possible real large 3D analyses in geomechanics with reasonably fine FE meshes.

It will also be important to note here that an essential feature of the modelling in geomechanics is the presence of some level of uncertainty in many input data, for example, in the described model, we can see some uncertainty in the values of the pre-mining stress, in modelling of the mining process with caving, in the size of zones with damaged rocks and properties of the goaf material and so on. For reliable modelling, this uncertainty must be treated by solution of several variants of the model and evaluation of the sensitivity to change of various parameters. This further increases the computing demands and emphasizes the needs for high performance solvers as well as for efficient preprocessors and postprocessors.

The performed work shows also some directions for further research.

1. Implementation and testing other high performance solvers which were already tested on smaller benchmark problems, see [20], [21], [22].

2. More deep study of the questions connected with the solution of singular systems. Because singularity is not numerically stable, we already tested some regularization of the problem, see [19]. Unfortunately, the existing preconditioner appeared as not very efficient for the regularized problem. Other possibility is a singularization of the problem as discussed in [3].

3. Testing the use of composite grid techniques for obtaining different levels of grid density. Note that for all geomechanical problems there are typically three levels of density: the highest density around the considered objects, modest density in a surrounding domain of interest and low density in the vicinity of the outer boundary of the problem domain which must be large due to outer boundary conditions.

4. Investigation of other parallelization techniques connected with composite grids, displacement decomposition or some other artificial decomposition of the problem.

In the connection with the parallelization issues, we can mention one promising result obtained during solution of a regular positive definite system arising from FE analysis on the same FE grid [10]. For this problem, again with nearly 4 million of unknowns, the reduction of the computer times from 11.6 hour for sequential PCG-1 solver on IBM RS/6000 3CT to 1.3 hour for parallel PCG-PV solver on IBM SP-2 with 3 engaged processors was obtained. The exploited solver PCG-PV is based on inner-outer iteration variant of the displacement decomposition technique, see [8]. Unfortunately, this solver was not so successful for singular systems (stability problems due to singular preconditioner).

Acknowledgement

The support from the grants COPERNICUS 940820 of the European Commission and Grant GA ČR 105/95/1273 of the Grant agency of the Czech Republic and the possibility to use the IBM SP-2 system at VŠB - Technical University of Ostrava for the experiments with parallel computations are gratefully acknowledged.

References

[1] O. Axelsson: Conjugate gradient type methods for unsymmetric and inconsistent systems of linear equations, Lin. Alg. Appl. 29(1980), 1–6

[2] O. Axelsson: Iterative solution methods, Cambridge Univ. Press, Cambridge 1994

[3] O. Axelsson, M. Neytcheva, B. Polman: An application of the bordering method to solve nearly singular systems, in Proc. seminar: Numerical Mathematics in Theory and Practice, Plzeň 1993

[4] R. Blaheta: Displacement decomposition – incomplete factorization preconditioning techniques for linear elasticity problems, Numer. Lin. Alg. Appl. 1(1994), 107-126

[5] R. Blaheta, R. Kohut: PCG–1 iterative solver, TR – DAM – 9501, IGAS Ostrava, 1995.

[6] R. Blaheta, R. Kohut: Benchmarks and programs for testing iterative solvers for 3D problems of geomechanics, TR – DAM – 9502, IGAS Ostrava, 1995

[7] R. Blaheta, O. Jakl, J. Starý: A parallel CG solver for FE analysis of 3D problems in geomechanics, in GEOMECHANICS'96, A.A. Balkema, Rotterdam 1997.

[8] R. Blaheta, O. Jakl, J. Starý: Parallel Implementation of the Displacement Decomposition Preconditioning for Elasticity, Iterative methods and parallel computing (IMPC'97), Milovy 1997

[9] R. Blaheta, O. Jakl, R. Kohut, A. Kolcun, J. Starý: IGAS collection of benchmarks, solvers and test results, TR–DAM 97–02, Institute of Geonics AS CR, Ostrava 1997.

[10] R. Blaheta, O. Jakl, R. Kohut, A. Kolcun, J. Malík, Z. Rakowski and A. Hájek: Mathematical Modelling of the Effects of a New Mining Technology at the Uranium Mine Dolní Rožínka, 4th HIPERGEOS workshop, Brussels 1997

[11] A. Hájek, Z. Rakowski: Mathematical models for development of mining technology, COPERNICUS 940820 Project Report, Ostrava, 1995

[12] A. Hájek, A. Kolcun, Z. Rakowski: Mathematical models for development of mining technology: Software testing and computational results. Midterm. report. COPERNICUS 940820 Project Report, Ostrava 1996.

[13] R. Kohut: Software module: Code for implementation of preconditioners, IGAS Ostrava, 1996.

[14] A. Kolcun: TGRID – 2 preprocessor for structured non–orthogonal 3D finite element grids, TR-DAM 97-01, IGAS Ostrava, 1997

[15] L. Staš et al.: In situ measurements of the horizontal stresses at the Rožná deposit by the method of hydrofracturing. Technical Report, IGAS Ostrava, April 1997

[16] Z. Rakowski: Mining of large ore bodies by underhand slicing with caving under artificial roof without limitation of worked height in Rožná deposit. Technical report, IGAS Ostrava, 1994 (In Czech)

[17] R. Trueman: The application of a numerical model to longwall coal mine roadway design, Mining Science and Technology, 10(1990), 157-165.

[18] Y. Notay: Solving positive (semi) definite linear systems by preconditioned iterative methods, in Preconditioned Conjugate Gradient Methods, O. Axelsson, L. Yu. Kototilina (eds.), LNM 1457, Springer–Verlag, Berlin 1990.

[19] J. Nečas, I. Hlaváček: Mathematical theory of elastic and elasto-plastic bodies, Elsevier, Amsterdam 1981

[20] Z. Kestřánek: Tests and improvements of the FEC code, HIPERGEOS Workshop, Brussels 1997

[21] M. Neytcheva and B. Polman: Comparisons of various preconditioning techniques to solve iteratively the 3D linear elasticity problems, HIPERGEOS Workshop, Brussels 1997

[22] P. Saint Georges, R. Valkenberg : Benchmarking for HIPERGEOS – Part 1. TR - SMC 96/04, ULB Brussels 1996

Appendix 1

CONVERGENCE HISTORY FOR PCG-1 AND PCG-P SOLVERS

STEP 1 **

#EQUATIONS = 3873264

IT	RES	CONV.F.	A.CONV.F.	PC.RES	RES/RHS
1	.25655E+07	.43844E+00	.43844E+00	.18976E+05	.17913E+01
10	.60820E+06	.98813E+00	.79741E+00	.25908E+04	.42466E+00
20	.42067E+06	.97277E+00	.87667E+00	.16429E+04	.29373E+00
30	.34729E+06	.99479E+00	.91015E+00	.11077E+04	.24249E+00
40	.18317E+06	.94937E+00	.91704E+00	.62383E+03	.12789E+00
50	.15255E+06	.98845E+00	.92966E+00	.45029E+03	.10652E+00
60	.74819E+05	.93157E+00	.92992E+00	.23304E+03	.52241E-01
70	.39910E+05	.94046E+00	.93123E+00	.11271E+03	.27866E-01
80	.29592E+05	.99635E+00	.93605E+00	.85259E+02	.20662E-01
90	.37647E+05	.10159E+01	.94547E+00	.10485E+03	.26286E-01
100	.31093E+05	.98462E+00	.94897E+00	.87532E+02	.21710E-01
110	.24320E+05	.95132E+00	.95138E+00	.65825E+02	.16981E-01
120	.12029E+05	.92920E+00	.94975E+00	.32767E+02	.83989E-02
130	.67273E+04	.93958E+00	.94927E+00	.19002E+02	.46972E-02
140	.43440E+04	.97258E+00	.94983E+00	.11590E+02	.30331E-02
150	.34907E+04	.97232E+00	.95171E+00	.91489E+01	.24373E-02
160	.24081E+04	.97788E+00	.95245E+00	.64357E+01	.16814E-02
170	.14636E+04	.93273E+00	.95239E+00	.38955E+01	.10219E-02
172	.13762E+04	.96968E+00	.95258E+00	.34574E+01	.96089E-03

STEP 2 **

#EQUATIONS = 3873264

IT	RES	CONV.F.	A.CONV.F.	PC.RES	RES/RHS
1	.30251E+05	.57835E+00	.57835E+00	.26980E+03	.21122E-01
10	.70409E+04	.87471E+00	.81829E+00	.46557E+02	.49162E-02
20	.25767E+04	.92680E+00	.86025E+00	.14972E+02	.17991E-02
30	.17582E+04	.97095E+00	.89307E+00	.92742E+01	.12276E-02
36	.13766E+04	.96023E+00	.90390E+00	.69038E+01	.96115E-03

STEP 3 **

#EQUATIONS = 3873264

IT	RES	CONV.F.	A.CONV.F.	PC.RES	RES/RHS
1	.29801E+05	.60842E+00	.60842E+00	.23366E+03	.20808E-01
10	.65387E+04	.85058E+00	.81761E+00	.43537E+02	.45655E-02
20	.23235E+04	.92032E+00	.85863E+00	.12985E+02	.16223E-02
28	.14257E+04	.94984E+00	.88134E+00	.74578E+01	.99544E-03

STEP 4 ***

#EQUATIONS = 3873264

IT	RES	CONV.F.	A.CONV.F.	PC.RES	RES/RHS
1	.35416E+05	.50220E+00	.50220E+00	.29536E+03	.24729E-01
10	.10261E+05	.86030E+00	.82468E+00	.67304E+02	.71644E-02
20	.51886E+04	.94961E+00	.87768E+00	.29297E+02	.36228E-02
30	.34818E+04	.95505E+00	.90459E+00	.18868E+02	.24311E-02
40	.23065E+04	.96796E+00	.91805E+00	.11093E+02	.16104E-02
50	.17800E+04	.97035E+00	.92906E+00	.80610E+01	.12429E-02
60	.14290E+04	.97691E+00	.93708E+00	.61896E+01	.99776E-03